MAIT cells and MR1 play an immunosuppressive role in glioblastoma through the induction of neutrophils and MDSCs

Taijun Hana and Masaki Terabe

Basic Immunology Section, Neuro-Oncology Branch, National Cancer Institute, National Institutes of Health, Bethesda, MD, USA

Running title:

Immunosuppressive role of MAIT cell and MR1 in GBM

Corresponding:

Masaki Terabe, Ph.D, Basic Immunology Section, Neuro-Oncology Branch, National Cancer Institute, National Institutes of Health, Building 37, Room 1016, 37 Convent Drive, Bethesda, MD 20892, USA

Tel: 240-760-6731

E-mail: terabe@mail.nih.gov

Funding: This work was supported by the intramural program of the National Institutes of Health, National Cancer Institute, Center for Cancer Research (ZIA BC 011877).

Conflict of Interest: The authors have no conflicts of interest to declare.

24 **Authorship:** Conception and design: T.H, M.T. Data analysis: T.H. Manuscript writing: T.H.,

25 M.T. Final approval: All authors approved.

26

Abstract

Background: Major histocompatibility complex class I-related protein (MR1) is an antigen-presenting molecule for Mucosal-Associated Invariant T (MAIT) cells. Although the expression level of the *MR1* gene was reported to correlate with worse survival in glioma patients, a detailed mechanism of this association has not been elucidated. This study aimed to understand the mechanism by which *MR1* levels affect glioblastoma (GBM) patient survival and any potential involvement of MAIT cells in this mechanism.

Methods: Multi-layered gene expression analysis, including direct sequence alignment and search, were conducted on The Cancer Genome Atlas (TCGA)-GBM data. The immunological impact of MAIT cells in GBM was evaluated using multiple analytical methods, including statistical correlation analysis and Gene Set Enrichment Analysis. Pan-cancer TCGA data was utilized to evaluate the role of MAIT cells in other cancers.

Results: Intact *MR1* was expressed in a broad spectrum of cell types in GBM, and its expression level was inversely correlated with the survival of GBM patients. Significant positive correlations were found between the expression of *MR1*, the amount of MAIT cell infiltration, and the activity of tumor-associated neutrophils (TANs)/myeloid-derived suppressor cells (MDSCs) in GBM. Simultaneously, the activity of TANs/MDSCs was significantly inversely correlated with the survival of GBM patients. Similar associations between MAIT/MR1 and TANs/MDSCs were observed in four additional cancer types.

Conclusions: Our observations shed light on the possible immunosuppressive role of MAIT cells and MR1 in GBM. It was indicated that *MR1* up-regulation leads to activation of MAIT cells, which in turn induce the activation and infiltration of TANs/MDSCs. Our results suggest the existence of a novel immunosuppressive MAIT/MR1-TAN/MDSC pathway whose activation

50 contributes to the poorer prognosis of GBM patients and which necessitates novel strategies to
51 counteract this immunosuppressive role of MAIT cells.
52
53 **Keywords:** Glioblastoma, MAIT cell, MR1, neutrophil, MDSC, immunosuppression
54
55 **Key points:**
56 - The expression level of *MR1* inversely correlates with the survival of GBM patients.
57 - *MR1* expression levels and MAIT cell infiltration correlated.
58 - MAIT cell and MR1 play immunosuppressive roles in GBM through neutrophil and MDSC.
59

60 **Importance of the study**

61 MR1-restricted MAIT cells are unconventional T cells that have the potential to regulate tumor
62 immunity. However, their immunobiology in GBM has not been understood. *MR1* expression
63 levels were reported to correlate with worse survival in glioma patients, while the involvement of
64 MAIT cells in the correlation was not clear. Using the TCGA-GBM data, we observed a fraction
65 of GBM patients have MAIT cells in the tumor and significant correlations between the expression
66 level of MR1, MAIT cell infiltration, and activities of TANs/MDSCs. Genes involved in multiple
67 TAN/MDSC-mediated immunosuppressive pathways were upregulated in MAIT-positive patients.
68 Importantly, both *MR1* expression levels and TAN/MDSC activation negatively correlated with
69 patient survival. The results suggest the existence of a novel immunosuppressive MAIT/MR1-
70 TAN/MDSC pathway whose activation contributes to the poorer prognosis of GBM patients, and
71 which provides novel strategies to counteract immune suppression in GBM patients.
72

73 **Introduction**

74 Glioblastoma (GBM) is the most devastating and common primary brain tumor in adults.
75 Despite a multi-modal standard of care, which includes surgical resection followed by
76 radichemotherapy, five-year survival remains around 10%[1], underscoring the need for better
77 treatment. Immunotherapies, such as immune checkpoint blockers (ICB), have shown promise in
78 treatments of other cancer types, but to date have not shown clinical efficacy in the treatment of
79 GBM[2]. This lack of efficacy has been attributed to a highly immunosuppressive microenvironment,
80 which includes a high content of immunosuppressive myeloid cells[3]. However, factors that activate
81 or induce those immunosuppressive myeloid cells are still under investigation.

82 Numerous studies are underway to elucidate mechanisms of immunosuppression in GBM.
83 Recently, it was reported that a transcriptomic expression level of major histocompatibility
84 complex class I-related protein (MR1) significantly correlated to the poor survival of glioma
85 patients[4]. However, the underlying mechanism by which the *MR1* expression level correlates with
86 poor survival was not fully determined. MR1 is a non-classical major histocompatibility complex
87 (MHC) class I protein and is the antigen-presenting molecule for Mucosal-Associated Invariant T
88 (MAIT) cells. The only known function of MR1 is antigen presentation to MAIT cells. MR1 has
89 been found in almost all mammals, and its genome sequence is highly conserved in many species,
90 suggesting the importance of MR1 across the mammalian kingdom. The repertoire of antigens
91 presented by MR1 is, however not well understood. It has been shown that riboflavin-derivatives,
92 bacterial metabolites, are a major type of antigen presented to MAIT cells. However, it was
93 recently reported that MR1 might load undefined cancer-derived antigens and present them to
94 MR1-restricted T cells[5]. MAIT cells express an invariant T cell receptor (TCR) alpha chain, which
95 utilizes Vα7.2Jα33 in humans[6]. Currently, several additional TCR gene segment combinations,

96 such as Vα7.2Jα12 and Vα7.2Jα20, have been reported for the invariant TCRα chain. Although
97 MAIT cells were discovered as a T cell population enriched in gut lamina propria, they are
98 prevalent in non-mucosal tissues in humans.

99 MAIT cells can secrete multiple cytokines upon their activation. They can secrete Th1-type
100 cytokines such as IFN-γ and TNF and Th17-type cytokines such as IL-17, IL-22, and IL-21. Their
101 cytokine profile can be modified depending on the environment they are in[7]. Although the
102 functions of each cytokine cannot be simply stated because of their complexity, the Th1-type
103 cytokines tend to produce immune responses needed for killing intracellular pathogens and cancer
104 cells. Th17-type cytokines induce immune responses against fungus infection. Among them, IL-
105 17 is known to promote the local attraction and activation of specific myeloid cells, such as
106 neutrophils, through the induction of chemokines[8,9].

107 The role of MAIT cells in cancer is uncertain, and there is no consensus on whether activated
108 MAIT cells are more likely to promote or inhibit cancer progression[7,10]. Since MAIT cells can also
109 secrete perforin and granzyme B, they can potentially lyse cancer cells. Some reports suggest that
110 MAIT cells can kill cancer cells including glioma-derived cells under certain *in vitro* conditions,
111 but their ability to target human cancers *in vivo* has not been confirmed[11,12]. On the other hand,
112 Yan, et al., using *in vivo* mouse tumor models, demonstrated that MAIT cells promote tumor
113 initiation, growth, and metastasis[13]. Some clinical studies reported an inverse correlation between
114 the number of tumor-infiltrating MAIT cells and survival in multiple types of cancer[14,15]. The
115 discrepancy in observed MAIT cell functions *in vitro* and *in vivo* or clinical conditions suggests
116 that the immunological functions of MAIT cells can be modified by their surrounding environment.
117 Interaction between GBM and MAIT cells has not been well studied. Peterfalvi, et al., using RT-

118 PCR, suggested the infiltration of MAIT cells in clinical GBM samples, but their clinical impact
119 or function in GBM remained to be elucidated[16].
120 We explored the roles of MR1 and MAIT cells in GBM by using large patient cohort data sets.
121 We found a significant correlation between *MR1* expression and GBM patients' poor survival and
122 significant correlations among *MR1*, MAIT cells, and the activity of tumor-associated neutrophils
123 (TANs)/myeloid-derived suppressor cells (MDSCs). Based on the findings, we propose a
124 hypothesis that *MR1* up-regulation with infiltration of MAIT cells in GBM activates
125 TANs/MDSCs that express multiple immunosuppressive mechanisms. The MAIT/MR1-
126 TAN/MDSC pathway can be a mechanism that contributes to the lack of effective response to
127 immunotherapy and provides the poor prognosis of GBM.
128
129 **Results**
130 ***MR1* expression levels correlated with worse overall survival of GBM patients**
131 The Cancer Genome Atlas (TCGA)-GBM expression data showed that *MR1* expression levels
132 varied among the patient-derived GBM samples (Figure_1a). We then examined the correlation
133 between *MR1* expression levels and GBM patients' overall survival. We used data from TCGA
134 and the Chinese Glioma Genome Atlas (CGGA)[17] and observed a significant negative correlation
135 between *MR1* expression levels and GBM survival (Figure_1b), with higher expressions of *MR1*
136 being associated with worse survival, in agreement with the previously reported prognostic value
137 of *MR1* expression in GBM[4]. We also investigated whether the observed association could be
138 attributed to functional mutations in *MR1* including the recently-reported loss of antigen
139 presentation function of the substitution (*MR1*-R31H) in a human patient[18], but found a very low
140 frequency (0.06%) of genomic mutations in a range of glioma data sets including 3391 glioma

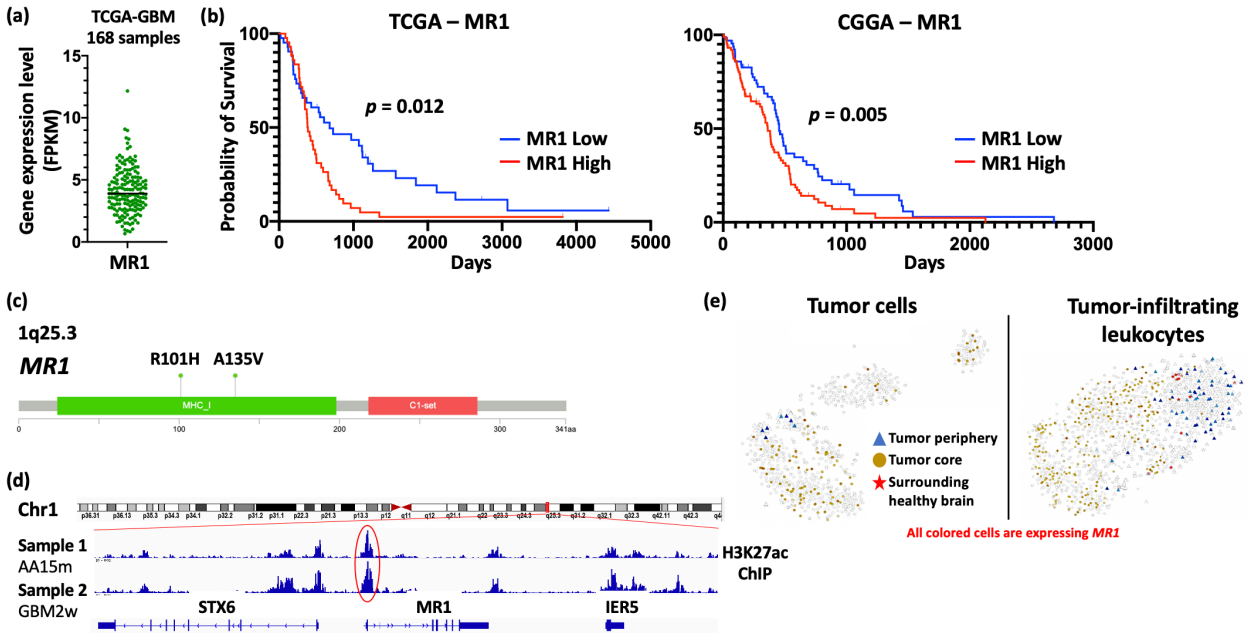

Figure_1: The *MR1* gene status and its prognostic correlation in GBM

(a) The RNA-expression data of TCGA-GBM 168 core samples were analyzed to see the expression levels of *MR1*. (b) The correlation between *MR1* expression and GBM patient survival. Clinical data available TCGA-GBM 153 patient data and Chinese Glioma Genome Atlas (CGGA) 85 primary GBM patient data were analyzed. Cut off FPKM: TCGA-MR1 = 3.67, CGGA-MR1 = 9.59, Log-rank test (c) The mutational schema of *MR1* locus in 3391 samples of glioma. Only 2 missense mutations were detected. (d) H3K27ac ChIP viewer image in *MR1* locus of GBM and high-grade glioma samples, GBM2w (IDHwt GBM, GSM1824806), AA15m (IDHmut-R132H, Grade3 Astrocytoma, GSM1824808). (e) Single-cell RNA-seq data of 3589 cells from GBM tissues of four patients were analyzed with a tSNE plot. All colored dots represent cells expressing *MR1*.

141 samples, and none of which had the reported loss of function mutation *MR1*-R31H (Figure_1c).

142 Additionally, we examined the epigenetic transcription status of *MR1* using available H3K27ac

143 ChIP data[19] of GBM and grade 3 astrocytoma, and found that the *MR1* promotor was active across

144 these samples (Figure_1d). Given the bulk tissue nature of TCGA samples, we also considered

145 whether the *MR1* expression in a subset of the samples could be due to the larger contribution of

146 micro-environment components in those samples. We utilized single-cell RNA-sequencing (RNA-

147 seq) data[20] and found that *MR1* was widely expressed in both glioma cells and tumor-infiltrating

148 leukocytes (TILs) in GBM(Figure_1e), and that *MR1* expression was relatively upregulated in the
149 tumor core compared to the tumor periphery.
150 All these observations indicated that intact *MR1* is widely transcribed in GBM tissue and
151 suggested that it is involved in the tumor pathogenesis of GBM.
152
153 **The level of *MR1* expression correlates with the activity of TANs and MDSCs**
154 To elucidate a potential mechanism to explain the correlation between high *MR1* expression
155 and poor prognosis, we extracted the top 500 significantly co-expressing genes (Supplementary
156 table_1) of *MR1* by using TCGA-GBM gene expression data. We further analyzed those 500 genes
157 for correlations with clinical outcomes[21]. Among the top 500 genes co-expressed with *MR1,* 158
158 genes significantly correlated with disease prognosis (Supplementary table_2) (Figure_2a). The
159 pathway analysis of the 158 genes showed strong enrichment (q < 2.0 x 10e-10) of the neutrophil
160 degranulation pathway (R-HSA-6798695) (Figure_2b). Since neutrophil degranulation (ND)
161 results from neutrophil activation, this data indicated that intra-tumoral *MR1* up-regulation
162 correlates with neutrophil activation in GBM tissue, which could impact the clinical prognosis.
163 Thirty genes (Supplementary table_3) among the 158 genes were classified into the ND pathway,
164 and we call these 30 genes ND30. It is known that the biological characteristics of tumor infiltrated
165 neutrophils and blood circulating neutrophils are significantly different because the tumor
166 microenvironment modifies their activities[22]. Thus, tumor infiltrated neutrophils are typically
167 called tumor-associated neutrophils (TANs). Since we focused on tumor-derived transcriptomic
168 data, all neutrophils in this study will be called TANs. Recently, it was reported that ND pathway
169 genes were also up-regulated in activated myeloid-derived suppressor cells (MDSCs)[23]. Thus, the
170 observed up-regulation of the ND pathway can be an indication of MDSC activation as well.

171 Additionally, it is also known that TANs and MDSCs share many morphological, functional, and

172 transcriptomic characteristics and are difficult to distinguish from each other[24,25]. Therefore, the

173 activities of TANs and MDSCs were evaluated simultaneously in the current study.

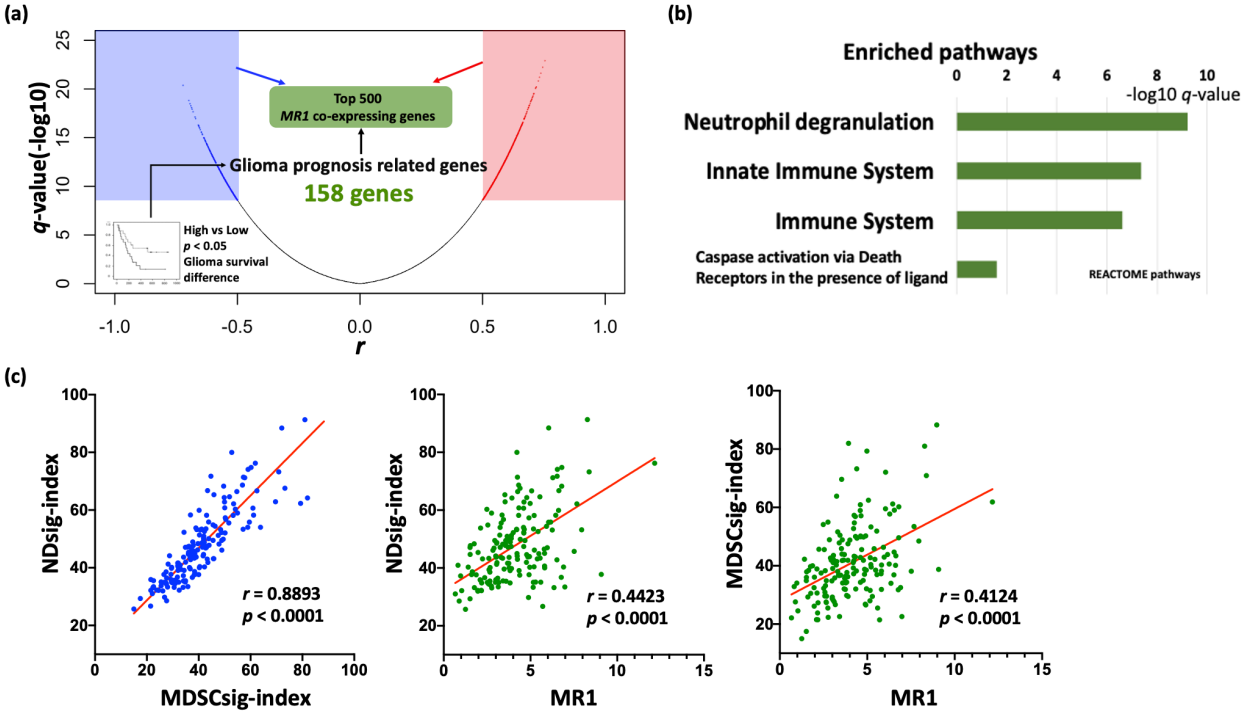

Figure_2: Correlations of *MR1* expression and the activity of TANs/MDSCs
(a) A schematic illustration of the extracted top 500 significantly co-expressing genes with *MR1* and the prognosis related 158 genes among them. The horizontal axis is the Spearman's *r* values for each gene's correlation level with *MR1*, and the vertical axis is the *q*-value (Benjamini-Hochberg adjusted *p*-value) for each gene. (b) The enriched pathways of the 158 genes. The bar graph shows the enriched *q*-values for each pathway. (c) Correlation scatter plots between *MR1* gene expression, NDsig-index, and MDSCsig-index among the 168 TCGA-GBM samples.

174 To examine the correlation between the activities of TANs and MDSCs in GBM, we calculated

175 the ND signature gene index (NDsig-index, as the average fragments per kilobase of transcript per

176 million mapped fragments, FPKM, of the 479 genes of ND pathway signature, R-HSA-6798695,

177 Supplementary table_3) and MDSC-signature gene[26] index (MDSCsig-index, as the average

178 FPKM of the 80 MDSC-signature genes, Supplementary table_3) for each GBM sample.

179 Interestingly, those two scores among samples were highly correlated (Spearman's $r = 0.889$, $p <$

180 0.0001), and significant correlations between *MR1* and MDSCsig-index and *MR1* and NDsig-
181 index were also confirmed (Figure_2c). These data suggest that the *MR1* and the activity of
182 TANs/MDSCs in GBM samples are highly correlated, and the up-regulation of *MR1* possibly
183 induces the activation of TANs/MDSCs.
184
185 **MAIT cell infiltrated GBM samples had a significantly higher level of *MR1* expression**
186 Since MR1 is an antigen-presenting molecule for MAIT cells, presumably, there is no direct
187 interaction between MR1 and TANs/MDSCs. Thus, we hypothesized that MAIT cells are involved
188 in the MR1-TAN/MDSC pathway that negatively impacts GBM prognosis. One previous study
189 reported on the MAIT cell infiltration into GBM, but the results have not been verified by
190 multifaceted analysis[16]. To detect MAIT cell infiltration into GBM, we took advantage of the
191 expression of a unique invariant T cell receptor alpha chain, which utilizes a Vα7.2 (TRAV1-2)
192 gene segment combined with either a Jα33 (TRAJ33), a Jα12 (TRAJ12), or a Jα20 (TRAJ20) gene
193 segment, by MAIT cells. The raw-sequence FASTQ files of TCGA-GBM samples were
194 comprehensively searched to find the characteristic sequences for the gene segments of TRAV1-
195 2, TRAJ33, TRAJ12, and TRAJ20. The samples containing the reads of TRAV1-2 and one of
196 TRAJ33, TRAJ12, or TRAJ20 simultaneously were considered positive for MAIT cell infiltration.
197 Fourteen out of the 168 (8.3%) TCGA-GBM samples were identified as "MAIT-positive" samples
198 (Figure_3a, Supplementary table_4). We then evaluated the transcriptomic expression of the
199 MAIT cell surface receptors. Since CCR5, CCR6, CXCR6, CD161, IL-12R, and IL-18R are
200 known to be expressed in MAIT cells, we examined the expressions of these genes in comparison
201 with MAIT-positive/negative samples. All 6 genes had significant up-regulation in MAIT-positive
202 samples (Figure_3b). The gene expression of *IL17A*(IL-17), *TNF*, and *IFNG*(IFN-γ), which are

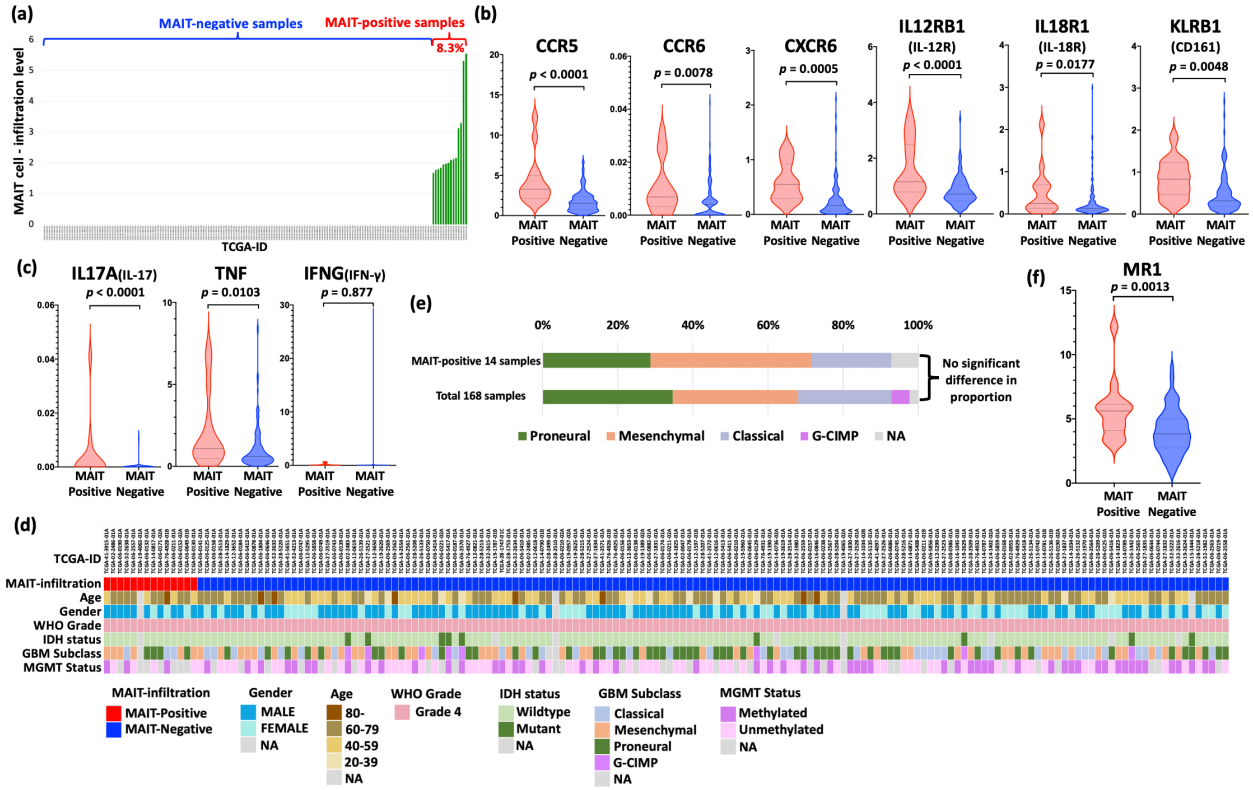

Figure_3: Multi-faceted evaluation of the MAIT infiltrated samples in TCGA-GBM
(a) The levels of MAIT-cell infiltration in TCGA-GBM samples. The 8.3% (14/168) of samples were detected as MAIT cell infiltration positive samples. The infiltration level was calculated with the formula, [The detected read count of the MAIT-target read of the sample/ The total RNA read count of the sample]. (b)(c) Violin plots showing the gene expression level of MAIT cell surface receptors/secreting cytokines. (d) The information on MAIT cell infiltration was integrated with other clinical/molecular indicators. Molecular indicators' information was obtained from a previously reported database[27], and the neural samples were integrated into the proneural samples. (e) The ratio-bar chart shows the distribution of GBM subtypes among MAIT-positive samples and the total TCGA-GBM samples. (f) A violin plot showing the *MR1* gene expression level in the MAIT positive/negative groups.

typical cytokines secreted by MAIT cells, was also examined. Significant up-regulation of *IL17A* and *TNF* in MAIT-positive samples was observed. However, no significant difference in *IFNG* expression was detected (Figure_3c). These data support our conclusion that samples containing transcripts of the invariant TCRα gene segment were infiltrated by MAIT cells. The cytokine gene expression data also raised the possibility that MAIT cells in GBM tissue may have a defect in producing IFN-γ.

209 The attributes of the MAIT-positive/negative samples were clarified as follows. Although there
210 was no isocitrate dehydrogenase (IDH) mutant case in MAIT-positive samples, there was no
211 statistically significant deviation in the distribution of the IDH mutant cases among the MAIT-
212 positive/negative samples (Binomial test, $p = 1$). Other indicators also did not differentiate the
213 MAIT-positive sample, and the MAIT-positive samples were statistically evenly distributed in
214 multiple GBM subtypes (Figure_3d, e). These findings indicate that MAIT cell infiltration is not
215 significantly associated with conventional attributes. We then examined the *MR1* expression status
216 of MAIT-positive samples and found that MAIT-positive samples had a significantly higher
217 expression level of *MR1* than MAIT-negative samples (Figure_3f). This important finding
218 indicates that the *MR1* up-regulation correlates with the increased MAIT cell infiltration into GBM
219 tissue.
220

221 **Multiple pathways of TANs/MDSCs contributed to the immunosuppression in MAIT-**
222 **positive samples**

223 To further understand the transcriptomic differences between MAIT positive and negative
224 samples, we conducted a comprehensive Gene Set Enrichment Analysis (GSEA) using Gene
225 Ontology Biological Process (GOBP) signatures. Interestingly, the most significantly enriched
226 process among all GOBP-processes, including non-immunological processes in MAIT-positive
227 samples, was an immunological process, the negative regulation of immune response
228 (GO:0050777) (Figure_4a). Since the negative regulation of immune response is an integrated
229 pathway including many immunosuppressive processes, this significant enrichment suggests that
230 multiple immunosuppressive mechanisms are more active in MAIT-positive samples than in
231 MAIT-negative samples. As described above, we observed that the *MR1* expression level

232 correlates with TAN/MDSC activation levels (Figure_2c). Thus, we extracted the neutrophil-
233 related pathways from all the pathways enriched in MAIT-positive samples. Many neutrophil
234 migration/chemotaxis and neutrophil activation-related pathways were significantly enriched in
235 MAIT-positive samples (Figure_4b). Since GOBP does not have appropriate MDSC-related
236 pathways, we could not examine the MDSC.

237 We next examined the TAN/MDSC activities in MAIT-positive/negative samples. The
238 expression levels of ND30 genes in MAIT-positive samples were clearly up-regulated compared
239 with in MAIT-negative samples (Figure_4c). We also calculated an "ND30-index", the mean
240 FPKM of the ND30 genes for each GBM sample, and the ND30-index showed a significantly
241 higher score in the MAIT-positive samples (Figure_4d). GSEA, using the signature genes of ND
242 pathway and the gene set of MDSC signature, showed significant enrichment of those signatures
243 in MAIT positive samples (Figure_4e). These data suggested that TANs/MDSCs are highly
244 activated in MAIT-positive samples compared with MAIT-negative samples.

245 TANs/MDSCs are known to suppress cancer immunity through various mechanisms[28-30]. For
246 instance, the up-regulation of arginase 1 (ARG1) expression depletes the local arginine[31], and the
247 low arginine level impairs T cells by down-regulating CD3 ζ chains, which are necessary for a
248 TCR signalling[32]. One of the other immunosuppressive mechanisms of TANs/MDSCs is through
249 the induction of $Foxp3^{+}CD4^{+}$ regulatory T cells (Treg). Tregs are attracted by CCL17 and CCL22
250 and induced by TGF-β[33]. CCL17 and TGF-β can be secreted by TANs[34,35] and MDSCs[36]. Although
251 TANs/MDSCs do not secrete CCL22 directly, they can contribute to its local up-regulation
252 through M2 macrophage polarization[37,38]. TANs/MDSCs also express PD-L1[39], and the up-
253 regulation of indoleamine 2,3-dioxygenase (IDO) depletes the local tryptophan and produces
254 kynurenine that inhibits T cell proliferation. The IL-10 and TGF-β produced by TANs/MDSCs

255 suppress T cell proliferation/activity as well[40-42]. We examined the gene expressions of those
256 molecules and found that all the genes were significantly up-regulated in MAIT-positive samples
257 compared with MAIT-negative samples (Figure_4f). We observed the up-regulation of *ARG1* and
258 the arginine reporter gene, *ASS1* (up-regulated upon the local arginine depletion), in MAIT-
259 positive samples (Figure_4g). Notably, *CCL17* in the MAIT-positive samples had an
260 approximately 10 times higher expression level on average compared with the MAIT-negative
261 samples. Increased Treg infiltration in MAIT-positive samples was indicated by a significant
262 increase of *FOXP3,* a typical Treg marker gene, in MAIT-positive samples (Figure_4h). CCR4, a
263 chemokine receptor expressed on Treg, which contributes to Treg-chemotaxis by binding to
264 CCL17, was also highly up-regulated in MAIT-positive samples (Figure_4h). Increased Treg
265 infiltration in MAIT positive samples was further confirmed using previously reported 22 Treg
266 signature genes[43] in GSEA （Supplementary table_3）(Figure_4i). These data suggested that the
267 multiple immunosuppressive pathways mediated by TANs/MDSCs were active in the MAIT-
268 positive samples. We then evaluated the impact of TANs/MDSCs on the GBM clinical course
269 (Figure_4j). Significant negative correlations of TAN/MDSC activity with the overall survival
270 indicated that their activities have an unfavorable impact on the GBM malignancy.

271 Altogether, the data strongly suggested that MAIT cells activated by *MR1* up-regulation induce
272 the activation and infiltration of TANs/MDSCs, which exert multiple immunosuppressive
273 mechanisms in GBM.

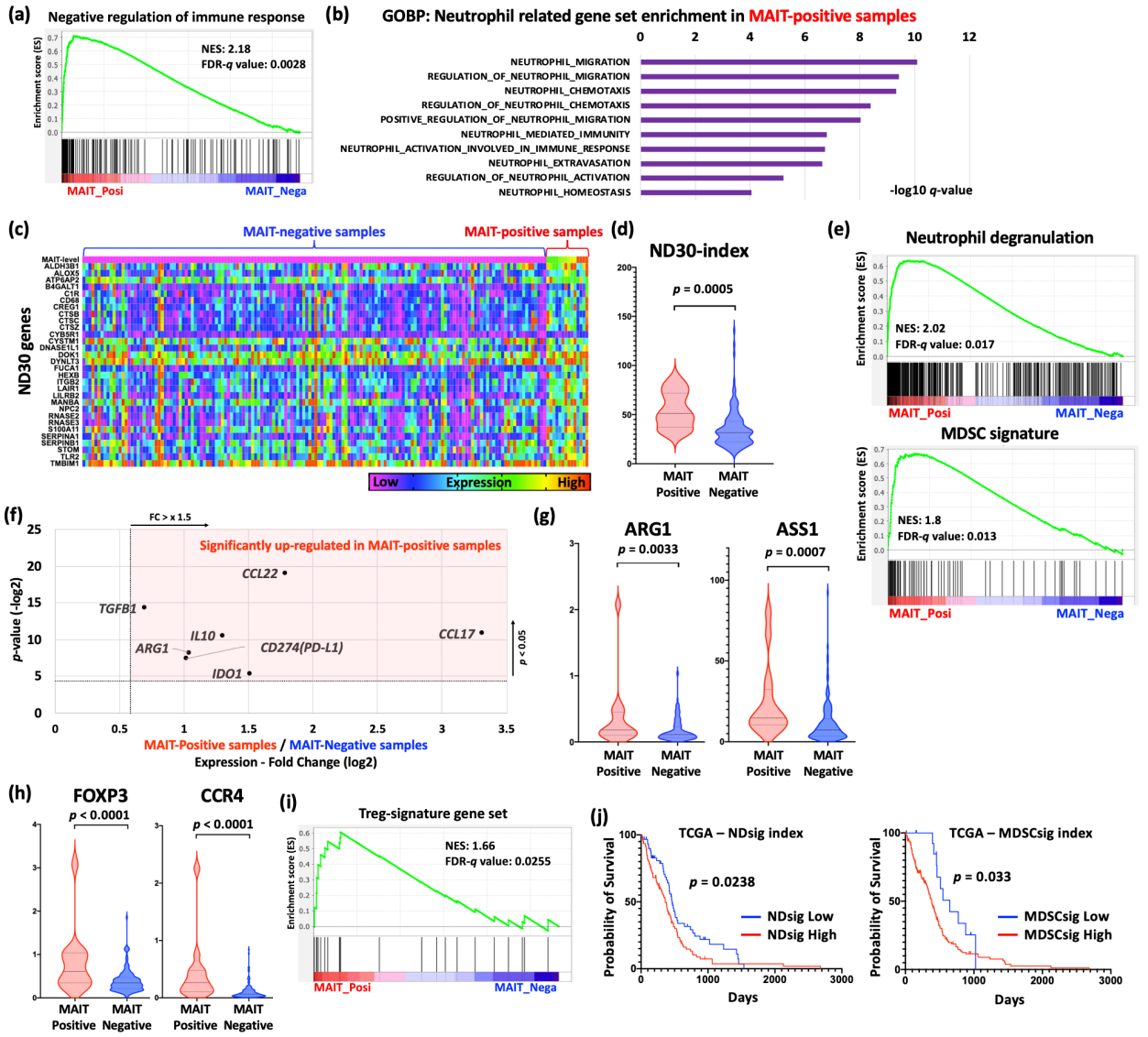

Figure_4: Evaluations of the activity of TANs/MDSCs in MAIT-positive/negative samples
(a) The enrichment plot of GSEA-GOBP's negative regulation of immune response in MAIT-positive/negative samples. (b) The enrichment results of neutrophil-related pathways in GSEA-GOBP in MAIT-positive samples. All pathways shown were significantly enriched ($q < 0.05$). (c) Heatmap of the gene expression level of ND30 genes for each sample. The vertical column represents one GBM sample. MAIT-positive samples were gathered on the right. (d) A Violin plot showing the ND30-index level. (e) GSEA enrichment plots of neutrophil degranulation pathway and MDSC signature. (f) Scatter chart showing the differential expression levels of the immunosuppressive pathway genes related to TANs/MDSCs among MAIT-positive/negative samples. The horizontal axis shows the fold change (log2 converted) as follows. [Mean FPKM of MAIT-positive samples / Mean FPKM of MAIT-negative samples] The vertical axis shows the *p*-value (-log2 converted) of the unpaired t-test that compares the expression levels of MAIT-positive/negative samples for the gene. (g) Violin plots showing the *ASS1* or *ARG1* gene expression level. (h) Violin plots showing the expression level of *FOXP3* and *CCR4*. (i) GSEA enrichment plot, using our Treg-signature gene set. (j) The prognostic correlation of NDsig-index

and MDSCsig-index with TCGA-GBM clinical data. Cut off: NDsig-index = 41.89, MDSCsig-index = 27.48, Log-rank test

274 **Pan-cancer analysis showed correlations between the activity of TANs/MDSCs and the**
275 ***MR1*'s prognostic correlation**

276 The results obtained by GBM gene expression data sets strongly suggested the existence of a
277 novel MAIT/MR1-TAN/MDSC pathway that potentially suppresses tumor immune responses. We
278 next asked if the correlations found in GBM can also be found in other types of cancer. In the
279 current study, we could not access to enough FASTQ raw data files to examine the MAIT cell
280 infiltration in different cancer types. Thus, we focused on investigating the relationship between
281 *MR1* expression and the prognosis of 14 major cancer types（breast cancer, cervical cancer,
282 colorectal cancer, head and neck cancer, liver cancer, lung cancer, melanoma, ovarian cancer,
283 pancreatic cancer, prostate cancer, renal cancer, stomach cancer, testis cancer, thyroid cancer）
284 using TCGA transcriptomic data for each cancer types. In 5 cancer types（colorectal cancer, head
285 and neck cancer, pancreatic cancer, stomach cancer, and testis cancer), high expression of *MR1*
286 was correlated with poor survival, whereas in 2 cancer types（lung cancer, renal cancer）the
287 relationship was reversed with expression levels of *MR1* positively correlated with survival
288 (Figure_5a). The remaining 7 cancer types had no significant difference in correlation with
289 prognosis. We call these 5 cancer types that *MR1* correlates with worse survival "MR1-
290 unfavorable cancers" and call the 2 cancer types that *MR1* correlates with better survival "MR1-
291 favorable cancers". These results suggested that the intra-tumoral biological pathways associated
292 with MR1 may be different among cancer types. As we evaluated previously, we examined the
293 transcriptomic expression of the MAIT cell surface receptor genes in the MR1-high/low groups of
294 these MR1-unfavorable/favorable cancers. In all seven cancer types, most of the MAIT-surface

295 genes were significantly up-regulated in the MR1-high group (Figure_S1). These findings suggest
296 that the increased level of *MR1* expression increased the amount of infiltrating MAIT cells.
297 We then asked if TANs/MDSCs are involved in the *MR1*-involving mechanism that
298 significantly correlates with the disease prognosis. We performed GSEA using the customized
299 signature gene set of NDsig genes and MDSCsig genes (Supplementary table_3) and found that 4
300 cancer types (colorectal cancer, pancreatic cancer, stomach cancer, and testis cancer) in MR1-
301 unfavorable cancers had significant (FDR-$q < 0.25$) or strong trend in up-regulation of both ND
302 and MDSC signatures in the MR1-high group (Figure_5b). On the other hand, the signatures were
303 not correlated with *MR1* expression levels in all MR1-favorable cancers (renal, and lung cancer)
304 and one MR1-unfavorable cancer (head and neck) (detailed results are in Supplementary table_5).
305 We confirmed this observation by using other signatures of GSEA, which was performed using
306 the GOBP signature, and all neutrophil-related pathways that were significantly enriched in each
307 *MR1* high group were extracted. The 4 cancer types, which had significant up-regulation of
308 TAN/MDSC activities along with *MR1* up-regulation, showed significant up-regulation of
309 multiple neutrophil-related pathways, such as positive regulation of neutrophil migration,
310 neutrophil extravasation, neutrophil activation involved in immune response, regulation of
311 neutrophil chemotaxis, neutrophil-mediated immunity, in MR1-high group (Figure_5c). In
312 contrast, head and neck, renal, and lung cancers indicated no significant up-regulation of
313 neutrophil-related pathways in the MR1-high or low group. These results well supported the
314 hypothesis that the MAIT/MR1-TAN/MDSC pathway is active in MR1-unfavorable cancers. It is
315 important to note that MAIT/MR1 did not correlate with TAN/MDSC activities in MR1-favorable
316 cancer types.

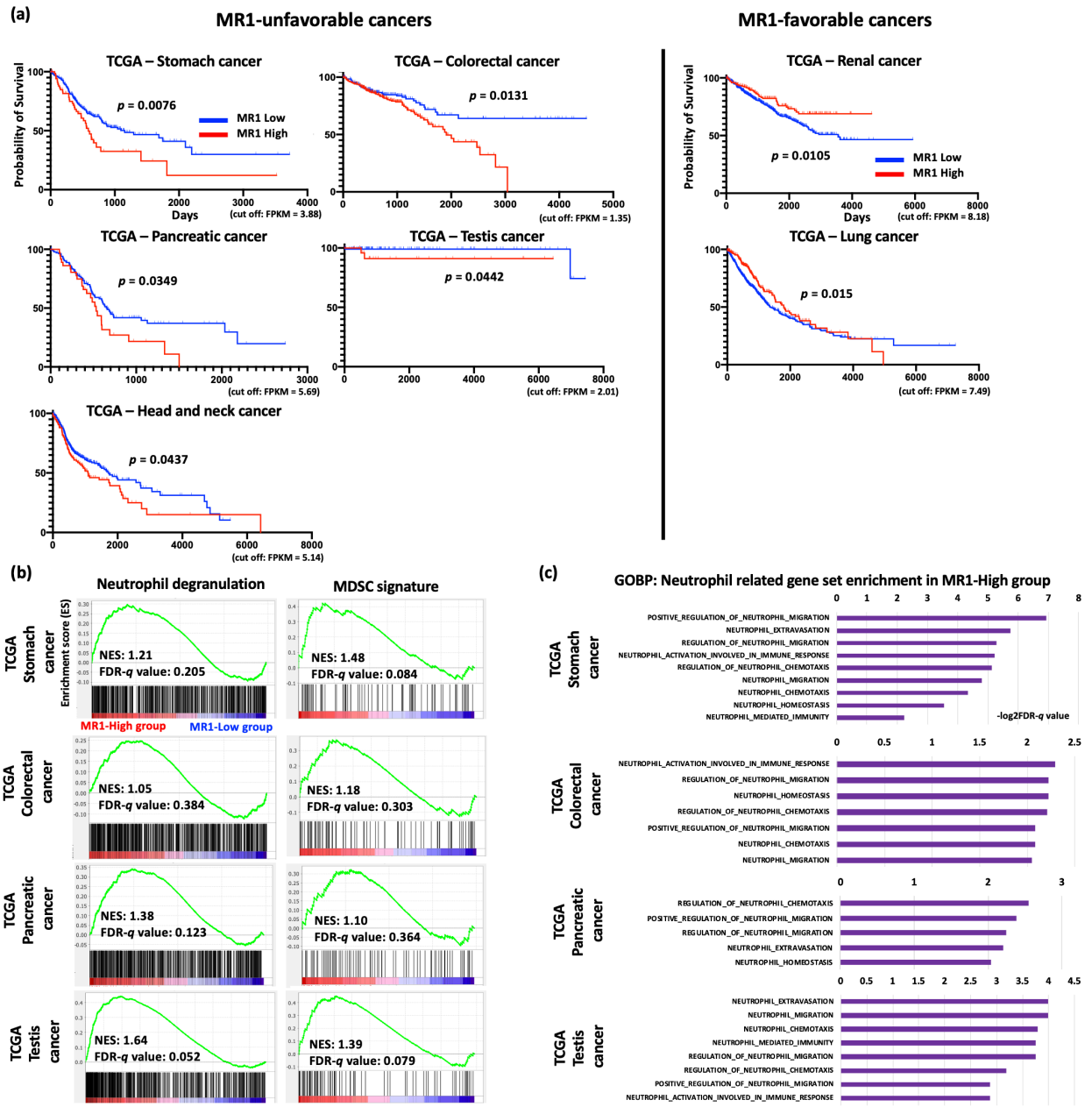

Figure_5: Correlations between *MR1*, prognosis, and TANs/MDSCs in the pan-cancer analysis

(a) The prognostic correlation of *MR1* in multiple cancer types. All red lines represent the MR1-high group, and blue lines represent the MR1-low group. (b) Enrichment plots of the GSEA using neutrophil degranulation pathway and our MDSCsig gene set for multiple cancer types. MR1-high/low groups were compared. (c) The enrichment results of neutrophil related pathways in GSEA-GOBP in the MR1-high group. All pathways shown were significantly enriched ($q < 0.05$).

317 **Discussion**

318 In this study, we proposed a novel MAIT/MR1-TAN/MDSC pathway as a potential
319 mechanism for a negative impact of *MR1* expression on GBM prognosis. To our knowledge, this
320 is the first study revealing the function of MAIT cells in glioblastoma. The transcriptional data of
321 TCGA-GBM revealed that high expression of *MR1* was significantly correlated with GBM's poor
322 survival. This observation was consistent with a previous report and was also confirmed by the
323 CGGA database[4]. Comprehensive gene expression data analysis and the direct search of the raw
324 sequence data of TCGA-GBM showed that 8.3% of the GBM samples had MAIT cell infiltration,
325 and the intra-tumoral *MR1* expression significantly correlated with the infiltration level of MAIT
326 cells. The GSEA, comparing the MAIT-positive/negative samples, showed that tumor immunity
327 in MAIT-positive samples was significantly negatively regulated, supporting an
328 immunosuppressive role of MAIT cells. Further analysis showed that the MAIT cell infiltration
329 was significantly correlated with the activity of the immunosuppressive cell population,
330 TANs/MDSCs. Simultaneously, TAN/MDSC activity was significantly correlated to the poor
331 survival of GBM. These data suggested that *MR1* up-regulation activates MAIT cells that
332 negatively impact the GBM prognosis through the activation of TANs/MDSCs. The pan-cancer
333 analysis also strongly suggested the activity of the MAIT/MR1-TAN/MDSC pathway in 4
334 additional cancer types.

335 There are ongoing debates about whether the MAIT cell is an ally or an enemy of cancer
336 immunity[10]. A few reports demonstrated that MAIT cells can kill cancer cells including glioma-
337 derived cells under limited experimental conditions[11,12]. However, this finding does not necessarily
338 mean that they can kill cancer cells *in vivo*. No studies based on clinical data or *in vivo* experiments
339 provided evidence of the tumor-suppressive ability of MAIT cells. On the contrary, their tumor-

340 promoting ability has been suggested by multiple reports based on clinical data and *in vivo*
341 models[13-15]. Duan, et al. showed the possibility that tumor-infiltrating MAIT cells are
342 reprogrammed in the tumor milieu to produce IL-8 and suppress the ability to produce IFN-γ and
343 IL-17[14]. Another study reported that tumor-infiltrating MAIT cells enhanced the production of IL-
344 17 and TNF-α while an IFN-γ production level was not changed[13]. In the current study, the
345 expression levels of *IL17A* and *TNF* were significantly higher in MAIT-positive samples while
346 there was no statistical difference in *IFNG* expression between MAIT-positive and negative
347 samples. Although details in altered functions of MAIT cells observed are different among studies,
348 it seems that a cytokine profile of MAIT cells in cancer-bearing individuals is skewed away from
349 type I immune response. The alteration of the IFN-γ producing function of MAIT cells seems to
350 be like what has been reported on another unconventional T cell, natural killer T (NKT) cells.
351 Dhodapkar M, et al. reported that the IFN-γ secreting ability of NKT cells circulating in
352 progressive cancer patients was suppressed[44].

353 Importantly, in renal and lung cancer, in which *MR1* expression levels correlated with better
354 prognosis, there was no correlation between *MR1* expression levels and the signatures of TANs or
355 MDSCs. This was in striking contrast to five cancer types including GBM, in which the disease
356 prognosis had a negative correlation with *MR1* expression levels. These data suggest that MAIT
357 cells have multiple faces in the context of the regulation of tumor immunity. Only when the
358 interplay between MAIT cells and TANs/MDSCs occurs do MAIT cells have a negative impact
359 on disease outcomes. There may be multiple factors that contribute to changing the roles of MAIT
360 cells among different cancer types. One factor may be the tumor microenvironment as each cancer
361 type has a different tumor microenvironment (TME) associated with MR1 and MAIT cells. Since
362 the immunological phenotype of MAIT cells can change depending on the environment[13,14], the

363 inter-cancer-type difference in TME possibly explains the different observations about
364 MAIT/MR1-TAN/MDSC pathway in multiple cancer types. MR1-favorable cancers, such as lung
365 cancer and renal cancer, may have a TME that does not guide MAIT cells towards the phenotype
366 that can affect TANs/MDSCs through the secretion of IL-17. TME may include antigens available
367 for MR1 to present to MAIT cells. Although it has been shown that vitamin B metabolites derived
368 from commensal bacteria are recognized by MAIT cells, there are yet to be characterized cancer-
369 derived antigens[5].

370 The level of TAN infiltration has been reported to correlate with the grades of glioma, and
371 some tumor-promoting mechanisms by TANs in GBM have been suggested[45-47]. However, the
372 mechanisms attracting TANs to the GBM tissue, and their activation mechanism are not well
373 understood. Our study observed a significant correlation between the amount of MAIT cell
374 infiltration and the activation level of TANs/MDSCs. MAIT cells rapidly secrete a large amount
375 of cytokines including IL-17[48], which is important in this context as it is well established that IL-
376 17 can promote the local attraction and activation of TANs through the induction of chemokines[8,9].
377 In fact, our data showed the significant up-regulation of *IL17A* in MAIT-positive samples, and not
378 only the activation of TANs/MDSCs but also multiple neutrophil attraction pathways were up-
379 regulated in MAIT-positive samples. Since neutrophils can exert strong cytotoxicity, they may
380 play anti-tumor roles. However, the biological function of neutrophils can be modified depending
381 on the tissue environment, especially by the local TGF-β status. Under a TGF-β depleted
382 environment, neutrophils tend to acquire the anti-tumor phenotype, called N1; whereas, under the
383 TGF-β sufficient environment, they tend to acquire the pro-tumor phenotype, called N2[29]. The
384 immunosuppressive and tumor-promoting role of N2-TAN has been reported in multiple cancer
385 types[29,30]. Since the expression level of *TGFB1* in MAIT-positive samples was significantly up-

386 regulated (Figure 4f), the TME of MAIT-positive patients is the preferred environment for TANs
387 to acquire the pro-tumor phenotype, N2. Thus, the TANs in MAIT-positive GBM samples are
388 considered to play a relatively immunosuppressive role and can be a cause of GBM's poor
389 prognosis.

390 MDSCs suppress cancer immunity[28] and in GBM, their immunosuppressive role and the
391 correlation between their infiltration and poor survival was reported[49]. He D, et al. showed that
392 MDSCs have phenotypic plasticity in their immunosuppressive function using *in vivo* cancer
393 model and IL-17 was required for the development of MDSCs in tumor-bearing mice and for
394 exerting MDSC's pro-tumor functions[50]. Guan X, et al. also observed a significant correlation
395 between the tumor IL-17 level and the MDSC infiltration level into renal cancer[51]. These reports
396 support our hypothesis that the IL-17 secreted from MAIT cells can attract MDSCs and promote
397 their immunosuppressive function in GBM.

398 We identified the samples with MAIT cell infiltration in TCGA-GBM by directly searching
399 TCR transcripts in the FASTQ files of their bulk RNA-seq. Only one previous report suggested
400 the presence of MAIT cells in GBM by detecting TCR transcripts by PCR with a limited number
401 of samples[16]. The present study is the first to use next-generation sequencer data for the purpose.
402 As a result, 8.3% of the samples were determined to have MAIT cell infiltration. Strictly, the
403 interpretation of this result must consider the limitation of bulk RNA-seq's resolution. Generally,
404 more than one hundred million cells can be included in a tumor sample submitted for bulk RNA-
405 seq[52], while the average total read (total of paired-end reads) per sample of TCGA-GBM was
406 approximately five hundred million reads. Hence on average, less than 5 reads for each cell may
407 be included in the bulk RNA-seq data, and only highly contained transcripts are detected. The
408 MAIT-positive samples we found should be considered a particularly high amount of MAIT-

409 infiltrated samples, and therefore it is likely that the method we used underestimated the number

410 of samples containing MAIT cells.

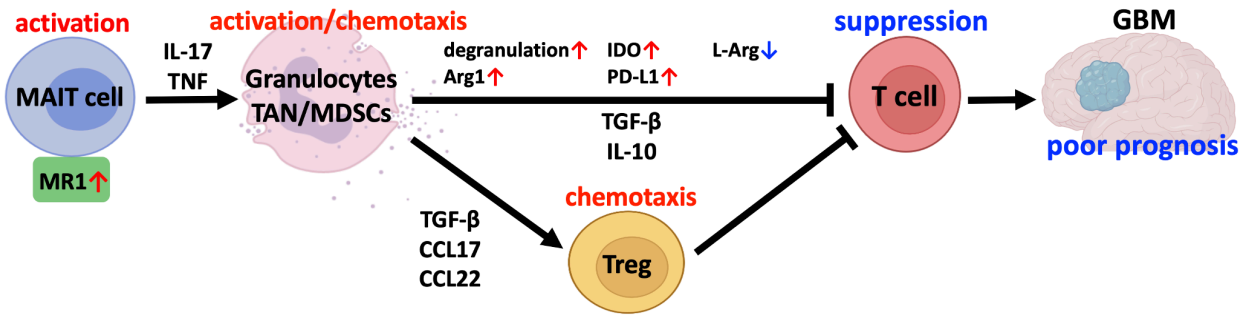

Figure_6: The MAIT/MR1-TAN/MDSC pathway
The activation of MAIT cell, along with the *MR1* up-regulation, activates and chemo-attracts granulocytes, such as TANs/MDSCs, through IL-17 and TNF production. The activated TANs/MDSCs induce Tregs via the production of TGF-β, CCL17, and CCL22, and Tregs suppress the T cell-mediated immunity. Simultaneously, TANs/MDSCs suppress T cells via multiple pathways. The suppression of T cell immunity provides a poor prognosis for GBM.

411 This study analyzed the clinical molecular data related to GBM, MR1, and MAIT cells based

412 on significant correlations in the context of disease outcomes. Hence, it is impossible to

413 definitively prove the direction of the causal relationship. For example, the correlation between

414 MAIT cells and TANs/MDSCs can also be interpreted as that TANs/MDSCs activated MAIT cells.

415 This point is one limitation of the current study. Although we proposed the mechanism that MAIT

416 cells can activate TANs/MDSCs via IL-17, there is the potential of some reverse pathways.

417 Another limitation of our study is that although most analyses were performed using transcriptomic

418 data for each cancer type, the transcriptomic levels do not always agree with the protein levels and

419 their functional status. MR1 is known to be expressed on the cell surface with the presence of

420 antigens. However, it does not function as antigen-presenting molecule when it is not loaded with

421 antigens even with their transcriptomic expression[53]. Therefore, ideally, comprehensive proteomic

422 data of a large GBM dataset should be analyzed for the purpose. However, such comprehensive

423 proteomics data for GBM is not currently available, thus we have leveraged the available data for
424 the analysis.

425 In conclusion, we propose a novel MAIT/MR1-TAN/MDSC pathway that can contribute to
426 the poor prognosis of GBM (Figure_6). MAIT cells can be a missing link between GBM and
427 TAN/MDSC's activation and infiltration, which was previously reported. Our study focused on *in*
428 *silico* analysis using cancer big data. Further research using experimental methods is needed to test
429 the hypothesis. However, our observations shed light on the possible immunosuppressive role of
430 MR1 and MAIT cells in GBM.

431

432 **Material and methods**

433 ***The definition of glioblastoma (GBM) in this study***

434 The WHO's central nervous tumor classification was revised in 2021, and IDH mutant grade 4
435 astrocytoma was excluded from the previously defined "glioblastoma"[54]. However, after
436 examining various data, we determined that it was not essential to divide the grade 4 gliomas into
437 multiple subtypes along with our study of MR1 and MAIT cells. We considered that the role of
438 MR1 and MAIT cells in glioma could be a consistent phenomenon in high-grade gliomas.
439 Therefore, our definition of GBM in this study is in line with the previous (WHO-2016) definition
440 of WHO. The disease concept is along with the TCGA-GBM dataset, in which GBMs are all the
441 grade 4 gliomas of IDH mutant and wild type.

442

443 ***Identification of MR1 mutational frequency, the epigenetic transcriptional status, the***
444 ***transcriptional distribution in GBM tissue***

445 The mutational frequency was confirmed using cBioportal[55]. A total of 3391 multi-grade glioma
446 samples were examined. The cBioportal's datasets of Glioblastoma (TCGA, Cell 2013), Low-
447 Grade Gliomas (UCSF, Science 2014), Merged Cohort of LGG and GBM (TCGA, Cell 2016),
448 Anaplastic Oligodendroglioma and Anaplastic Oligoastrocytoma (MSKCC, Neuro Oncol 2017),
449 Glioma (MSK, Nature 2019), Glioma (MSKCC, Clin Cancer Res 2019), Brain Lower Grade
450 Glioma (TCGA, PanCancer Atlas) were used. The H3K27ac ChIP data of GBM2w (IDHwt GBM,
451 GSM1824806), AA15m (IDHmut-R132H, Grade3 Astrocytoma, GSM1824808) were used to
452 examine the epigenetic transcriptional status of *MR1* in glioma. IgV_2.11.9 was used to visualize
453 the Bed.file data. Single-cell RNA-seq analyzing web tool, GBM-seq[20], was used to examine the
454 *MR1*'s transcriptional distribution in GBM tissue. The generated tSNE plot of *MR1* expression
455 analysis was used.
456
457 ***The TCGA gene expression analysis and the prognostic examination***
458 The TCGA-GBM core 168 samples'(Supplementary table_4) gene expression data was
459 downloaded from Genomic Data Commons Data Portal（https://portal.gdc.cancer.gov/）. All the
460 gene expression analyses were conducted using this set of data. Prognostic examinations with
461 specific gene expression in this study were done using the Log-rank test, and all cut-off thresholds
462 were decided using TCGA survival data analyzer[21,56]. TCGA prognostic analyses were conducted
463 using the TCGA-GBM 153 samples (Supplementary table_6) with available clinical data[21].
464 Chinese Glioma Genome Atlas (CGGA) data analysis was performed using the CGGA data
465 portal[17]. The dataset of "mRNAseq_325" was used with the order of *MR1* & survival analysis
466 option. The result of WHO grade IV survival (primary glioma) was used. When comparing specific
467 gene expressions between two groups, a two-tailed unpaired Student's t-test was used to analyze,

468 and $p < 0.05$ was considered statistically significant. When fold changes in gene expression were
469 calculated, the mean FPKM of both groups was used for the calculation. For pan-cancer analysis,
470 the TCGA expression and clinical data for all cancer types were obtained from The Human Protein
471 Atlas[21]. All analytical methods used are the same as GBM. All gene expression data analyzed in
472 this study was performed using an FPKM unit.
473
474 ***Extracting the MR1 co-expressing genes and gene set pathway analysis***
475 The *MR1* co-expressing genes were extracted with cBioportal using the RNA Seq V2 RSEM data
476 set of Glioblastoma Multiforme (TCGA, PanCancer Atlas, Cell 2018). "Co-expression" analysis
477 mode with "MR1" was conducted, and the top 500 co-expression genes were extracted. All the co-
478 expression or correlation analyses of this study were performed using Spearman's correlation test
479 using GraphPad Prism8(GraphPad Software, La Jolla, California, USA), and $p < 0.05$ was used as
480 the significant threshold. To extract the GBM prognosis-related genes from the top 500 *MR1* co-
481 expression genes, the GBM prognostic gene database[21] was utilized. The 158 genes significantly
482 correlating the poor survival of GBM ($p < 0.05$) were extracted (Supplementary table_2). Gene set
483 pathway analyses of this study were conducted with g:Profiler[57].
484
485 ***Analyses using the signature of Neutrophil degranulation, MDSC, and Treg***
486 The gene set of Neutrophil degranulation (REACTOME: R-HSA-6798695, 479 genes) was used
487 to generate the NDsig-index for each TCGA sample. All FPKM values of the 479 genes were
488 averaged for each sample, and the value was defined as NDsig-index for each sample. The MDSC
489 characteristic signature gene set was obtained from a previous study[26]. Since the gene set was
490 originally composed of 105 murine genes, we extracted 80 genes from them that exist in humans,

491 and the 80 genes were defined as MDSC signature genes (Supplementary table_3). The MDSCsig-
492 index was calculated similarly to the NDsig-index using the 80 MDSC signature genes. The
493 signature gene set for Treg was obtained from a previous study[43]. The 22 signature genes
494 differentially expressed in Tregs were used for our analysis (Supplementary table_3).
495
496 ***Detecting the MAIT-positive samples in TCGA-GBM***
497 All FASTQ files of 168 TCGA-GBM core samples were downloaded from the Genomic Data
498 Commons Data Portal Legacy Archive（https://portal.gdc.cancer.gov/legacy-archive/）. Access
499 to TCGA-controlled data and studies using them were approved by the National Cancer Institute
500 (#28406). Reads having the characteristic T cell receptor sequences (Supplementary table_7) of
501 MAIT cells were searched with the FASTQ files. It was confirmed that all the searched sequences
502 were unique in the whole genome, and no other loci have the same sequence using the GGGenome-
503 ultrafast sequence search (https://gggenome.dbcls.jp/en/). The samples containing the reads of
504 TRAV1-2 and TRAJ33 or TRAJ12 or TRAJ20 simultaneously were classified as the samples with
505 the MAIT cell infiltration and were defined as MAIT-positive. The MAIT-infiltration level of each
506 sample was calculated with the formula, [The detected read count of the TRAV1-2 read of the
507 sample/ The total RNA read count of the sample]. All these analyses were conducted on the NIH-
508 high performance computer, the Biowulf cluster system.
509
510 ***Gene expression heatmap and Gene Set Enrichment Analysis (GSEA)***
511 The FPKM values of ND30 genes for each sample were extracted to draw the heatmap of
512 Figure_4c. Intergenic normalization was performed with GraphPad Prism8(GraphPad Software,
513 La Jolla, California, USA), and each cell was colored along with the expression levels. GSEAs of

514 this study were conducted using the expression data of core 168 TCGA-GBM samples and the
515 pan-cancer samples. GSEA_4.2.3 was used to run the 1000 permutations analyses using the
516 signatures of c2.cp.reactome.v7.5.1.symbols.gmt, c5.go.bp.v7.5.1.symbols.gmt, and
517 c2.cp.kegg.v7.5.1.symbols.gmt. GSEA with the signature of ND, MDSC, and Treg was conducted
518 using our customized "gmx" signature files made from their characteristic signatures.
519

520 **Acknowledgments**

521 We thank Dr. Mark R. Gilbert and Dr. Orieta Celiku for the critical reading of the manuscript and
522 the NIH HPC group for providing the Biowulf cluster system. This work was supported by the
523 intramural program of the National Institutes of Health, National Cancer Institute, Center for
524 Cancer Research (ZIA BC 011877).
525

526 **References**

527 **1.** Stupp R, Taillibert S, Kanner A, et al. Effect of Tumor-Treating Fields Plus Maintenance
528 Temozolomide vs Maintenance Temozolomide Alone on Survival in Patients With
529 Glioblastoma: A Randomized Clinical Trial. *Jama.* 2017; 318(23):2306-2316.
530 **2.** Omuro A, Vlahovic G, Lim M, et al. Nivolumab with or without ipilimumab in patients
531 with recurrent glioblastoma: results from exploratory phase I cohorts of CheckMate 143.
532 *Neuro-oncology.* 2018; 20(5):674-686.
533 **3.** Klemm F, Maas RR, Bowman RL, et al. Interrogation of the Microenvironmental
534 Landscape in Brain Tumors Reveals Disease-Specific Alterations of Immune Cells. *Cell.*
535 2020; 181(7):1643-1660 e1617.
536 **4.** Kubica P, Lara-Velazquez M, Bam M, et al. MR1 overexpression correlates with poor
537 clinical prognosis in glioma patients. *Neuro-Oncology Advances.* 2021.
538 **5.** Crowther MD, Dolton G, Legut M, et al. Genome-wide CRISPR-Cas9 screening reveals
539 ubiquitous T cell cancer targeting via the monomorphic MHC class I-related protein
540 MR1. *Nature immunology.* 2020; 21(2):178-185.
541 **6.** Treiner E, Duban L, Bahram S, et al. Selection of evolutionarily conserved mucosal-
542 associated invariant T cells by MR1. *Nature.* 2003; 422(6928):164-169.
543 **7.** Cogswell DT, Gapin L, Tobin HM, McCarter MD, Tobin RP. MAIT Cells: Partners or
544 Enemies in Cancer Immunotherapy? *Cancers.* 2021; 13(7).
545 **8.** Parajuli P, Mittal S. Role of IL-17 in Glioma Progression. *J Spine Neurosurg.* 2013;
546 Suppl 1.
547 **9.** Wu L, Awaji M, Saxena S, Varney ML, Sharma B, Singh RK. IL-17-CXC Chemokine
548 Receptor 2 Axis Facilitates Breast Cancer Progression by Up-Regulating Neutrophil
549 Recruitment. *The American journal of pathology.* 2020; 190(1):222-233.
550 **10.** Haeryfar SMM, Shaler CR, Rudak PT. Mucosa-associated invariant T cells in
551 malignancies: a faithful friend or formidable foe? *Cancer Immunol Immunother.* 2018;
552 67(12):1885-1896.
553 **11.** Gherardin NA, Loh L, Admojo L, et al. Enumeration, functional responses and cytotoxic
554 capacity of MAIT cells in newly diagnosed and relapsed multiple myeloma. *Scientific*
555 *reports.* 2018; 8(1):4159.
556 **12.** Priya R, Brutkiewicz RR. MR1 Tetramer-Based Artificial APCs Expand MAIT Cells
557 from Human Peripheral Blood That Effectively Kill Glioblastoma Cells.
558 *Immunohorizons.* 2021; 5(6):500-511.
559 **13.** Yan J, Allen S, McDonald E, et al. MAIT Cells Promote Tumor Initiation, Growth, and
560 Metastases via Tumor MR1. *Cancer discovery.* 2020; 10(1):124-141.
561 **14.** Duan M, Goswami S, Shi JY, et al. Activated and Exhausted MAIT Cells Foster Disease
562 Progression and Indicate Poor Outcome in Hepatocellular Carcinoma. *Clinical cancer*
563 *research : an official journal of the American Association for Cancer Research.* 2019;
564 25(11):3304-3316.
565 **15.** Zabijak L, Attencourt C, Guignant C, et al. Increased tumor infiltration by mucosal-
566 associated invariant T cells correlates with poor survival in colorectal cancer patients.
567 *Cancer Immunol Immunother.* 2015; 64(12):1601-1608.
568 **16.** Peterfalvi A, Gomori E, Magyarlaki T, et al. Invariant Valpha7.2-Jalpha33 TCR is
569 expressed in human kidney and brain tumors indicating infiltration by mucosal-associated
570 invariant T (MAIT) cells. *Int Immunol.* 2008; 20(12):1517-1525.

571 **17.** Zhao Z, Zhang KN, Wang Q, et al. Chinese Glioma Genome Atlas (CGGA): A
572 Comprehensive Resource with Functional Genomic Data from Chinese Glioma Patients.
573 *Genomics Proteomics Bioinformatics.* 2021; 19(1):1-12.
574 **18.** Howson LJ, Awad W, von Borstel A, et al. Absence of mucosal-associated invariant T
575 cells in a person with a homozygous point mutation in MR1. *Sci Immunol.* 2020; 5(49).
576 **19.** Flavahan WA, Drier Y, Liau BB, et al. Insulator dysfunction and oncogene activation in
577 IDH mutant gliomas. *Nature.* 2016; 529(7584):110-114.
578 **20.** Darmanis S, Sloan SA, Croote D, et al. Single-Cell RNA-Seq Analysis of Infiltrating
579 Neoplastic Cells at the Migrating Front of Human Glioblastoma. *Cell reports.* 2017;
580 21(5):1399-1410.
581 **21.** Uhlen M, Zhang C, Lee S, et al. A pathology atlas of the human cancer transcriptome.
582 *Science (New York, N.Y.).* 2017; 357(6352).
583 **22.** Mollinedo F. Neutrophil Degranulation, Plasticity, and Cancer Metastasis. *Trends*
584 *Immunol.* 2019; 40(3):228-242.
585 **23.** Dean MJ, Ochoa JB, Sanchez-Pino MD, et al. Severe COVID-19 Is Characterized by an
586 Impaired Type I Interferon Response and Elevated Levels of Arginase Producing
587 Granulocytic Myeloid Derived Suppressor Cells. *Frontiers in immunology.* 2021;
588 12:695972.
589 **24.** Zhou J, Nefedova Y, Lei A, Gabrilovich D. Neutrophils and PMN-MDSC: Their
590 biological role and interaction with stromal cells. *Semin Immunol.* 2018; 35:19-28.
591 **25.** Aarts CEM, Kuijpers TW. Neutrophils as myeloid-derived suppressor cells. *Eur J Clin*
592 *Invest.* 2018; 48 Suppl 2:e12989.
593 **26.** Alshetaiwi H, Pervolarakis N, McIntyre LL, et al. Defining the emergence of myeloid-
594 derived suppressor cells in breast cancer using single-cell transcriptomics. *Sci Immunol.*
595 2020; 5(44).
596 **27.** Brennan CW, Verhaak RG, McKenna A, et al. The somatic genomic landscape of
597 glioblastoma. *Cell.* 2013; 155(2):462-477.
598 **28.** Yang Y, Li C, Liu T, Dai X, Bazhin AV. Myeloid-Derived Suppressor Cells in Tumors:
599 From Mechanisms to Antigen Specificity and Microenvironmental Regulation. *Frontiers*
600 *in immunology.* 2020; 11:1371.
601 **29.** Masucci MT, Minopoli M, Carriero MV. Tumor Associated Neutrophils. Their Role in
602 Tumorigenesis, Metastasis, Prognosis and Therapy. *Frontiers in oncology.* 2019; 9:1146.
603 **30.** Michaeli J, Shaul ME, Mishalian I, et al. Tumor-associated neutrophils induce apoptosis
604 of non-activated CD8 T-cells in a TNFα and NO-dependent mechanism, promoting a
605 tumor-supportive environment. *Oncoimmunology.* 2017; 6(11):e1356965.
606 **31.** Grzywa TM, Sosnowska A, Matryba P, et al. Myeloid Cell-Derived Arginase in Cancer
607 Immune Response. *Frontiers in immunology.* 2020; 11:938.
608 **32.** Rodriguez PC, Zea AH, DeSalvo J, et al. L-arginine consumption by macrophages
609 modulates the expression of CD3 zeta chain in T lymphocytes. *Journal of immunology*
610 *(Baltimore, Md. : 1950).* 2003; 171(3):1232-1239.
611 **33.** Shen Y, Wei Y, Wang Z, et al. TGF-β regulates hepatocellular carcinoma progression by
612 inducing Treg cell polarization. *Cell Physiol Biochem.* 2015; 35(4):1623-1632.
613 **34.** Chu HW, Trudeau JB, Balzar S, Wenzel SE. Peripheral blood and airway tissue
614 expression of transforming growth factor beta by neutrophils in asthmatic subjects and
615 normal control subjects. *J Allergy Clin Immunol.* 2000; 106(6):1115-1123.

616 **35.** Zhou SL, Zhou ZJ, Hu ZQ, et al. Tumor-Associated Neutrophils Recruit Macrophages
617 and T-Regulatory Cells to Promote Progression of Hepatocellular Carcinoma and
618 Resistance to Sorafenib. *Gastroenterology.* 2016; 150(7):1646-1658.e1617.
619 **36.** Veglia F, Sanseviero E, Gabrilovich DI. Myeloid-derived suppressor cells in the era of
620 increasing myeloid cell diversity. *Nat Rev Immunol.* 2021; 21(8):485-498.
621 **37.** Sinha P, Clements VK, Bunt SK, Albelda SM, Ostrand-Rosenberg S. Cross-talk between
622 myeloid-derived suppressor cells and macrophages subverts tumor immunity toward a
623 type 2 response. *Journal of immunology (Baltimore, Md. : 1950).* 2007; 179(2):977-983.
624 **38.** Wei C, Yang C, Wang S, et al. M2 macrophages confer resistance to 5-fluorouracil in
625 colorectal cancer through the activation of CCL22/PI3K/AKT signaling. *OncoTargets*
626 *and therapy.* 2019; 12:3051-3063.
627 **39.** Ballbach M, Dannert A, Singh A, et al. Expression of checkpoint molecules on myeloid-
628 derived suppressor cells. *Immunol Lett.* 2017; 192:1-6.
629 **40.** Li F, Zhao Y, Wei L, Li S, Liu J. Tumor-infiltrating Treg, MDSC, and IDO expression
630 associated with outcomes of neoadjuvant chemotherapy of breast cancer. *Cancer biology*
631 *& therapy.* 2018; 19(8):695-705.
632 **41.** Taga K, Tosato G. IL-10 inhibits human T cell proliferation and IL-2 production. *Journal*
633 *of immunology (Baltimore, Md. : 1950).* 1992; 148(4):1143-1148.
634 **42.** Dahmani A, Delisle JS. TGF-β in T Cell Biology: Implications for Cancer
635 Immunotherapy. *Cancers.* 2018; 10(6).
636 **43.** Pesenacker AM, Wang AY, Singh A, et al. A Regulatory T-Cell Gene Signature Is a
637 Specific and Sensitive Biomarker to Identify Children With New-Onset Type 1 Diabetes.
638 *Diabetes.* 2016; 65(4):1031-1039.
639 **44.** Dhodapkar MV, Geller MD, Chang DH, et al. A reversible defect in natural killer T cell
640 function characterizes the progression of premalignant to malignant multiple myeloma.
641 *The Journal of experimental medicine.* 2003; 197(12):1667-1676.
642 **45.** Liang J, Piao Y, Holmes L, et al. Neutrophils promote the malignant glioma phenotype
643 through S100A4. *Clinical cancer research : an official journal of the American*
644 *Association for Cancer Research.* 2014; 20(1):187-198.
645 **46.** Sippel TR, White J, Nag K, et al. Neutrophil degranulation and immunosuppression in
646 patients with GBM: restoration of cellular immune function by targeting arginase I.
647 *Clinical cancer research : an official journal of the American Association for Cancer*
648 *Research.* 2011; 17(22):6992-7002.
649 **47.** Fossati G, Ricevuti G, Edwards SW, Walker C, Dalton A, Rossi ML. Neutrophil
650 infiltration into human gliomas. *Acta neuropathologica.* 1999; 98(4):349-354.
651 **48.** Dusseaux M, Martin E, Serriari N, et al. Human MAIT cells are xenobiotic-resistant,
652 tissue-targeted, CD161hi IL-17-secreting T cells. *Blood.* 2011; 117(4):1250-1259.
653 **49.** De Leo A, Ugolini A, Veglia F. Myeloid Cells in Glioblastoma Microenvironment. *Cells.*
654 2020; 10(1).
655 **50.** He D, Li H, Yusuf N, et al. IL-17 promotes tumor development through the induction of
656 tumor promoting microenvironments at tumor sites and myeloid-derived suppressor cells.
657 *Journal of immunology (Baltimore, Md. : 1950).* 2010; 184(5):2281-2288.
658 **51.** Guan X, Liu Z, Zhang J, Jin X. Myeloid-derived suppressor cell accumulation in renal
659 cell carcinoma is correlated with CCL2, IL-17 and IL-18 expression in blood and tumors.
660 *Adv Clin Exp Med.* 2018; 27(7):947-953.

661 **52.** Del Monte U. Does the cell number 10(9) still really fit one gram of tumor tissue? *Cell*
662 *cycle (Georgetown, Tex.).* 2009; 8(3):505-506.
663 **53.** McWilliam HEG, Villadangos JA. How MR1 Presents a Pathogen Metabolic Signature
664 to Mucosal-Associated Invariant T (MAIT) Cells. *Trends Immunol.* 2017; 38(9):679-689.
665 **54.** Louis DN, Perry A, Wesseling P, et al. The 2021 WHO Classification of Tumors of the
666 Central Nervous System: a summary. *Neuro-oncology.* 2021; 23(8):1231-1251.
667 **55.** Cerami E, Gao J, Dogrusoz U, et al. The cBio cancer genomics portal: an open platform
668 for exploring multidimensional cancer genomics data. *Cancer discovery.* 2012; 2(5):401-
669 404.
670 **56.** Budczies J, Klauschen F, Sinn BV, et al. Cutoff Finder: a comprehensive and
671 straightforward Web application enabling rapid biomarker cutoff optimization. *PloS one.*
672 2012; 7(12):e51862.
673 **57.** Raudvere U, Kolberg L, Kuzmin I, et al. g:Profiler: a web server for functional
674 enrichment analysis and conversions of gene lists (2019 update). *Nucleic acids research.*
675 2019; 47(W1):W191-w198.
676

677

678 **Figure legends**

679 **Figure_1**

680 **The *MR1* gene status and its prognostic correlation in GBM**

681 (a) The RNA-expression data of TCGA-GBM 168 core samples were analyzed to see the
682 expression levels of *MR1*. (b) The correlation between *MR1* expression and GBM survival.
683 Clinical data available TCGA-GBM 153 patients' data and Chinese Glioma Genome Atlas
684 (CGGA) 85 primary GBM patients' data were analyzed. Cut off FPKM: TCGA-MR1 = 3.67,
685 CGGA-MR1 = 9.59, Log-rank test (c) The mutational schema of *MR1* locus in 3391 samples of
686 glioma. Only 2 missense mutations were detected. (d) H3K27ac ChIP viewer image in *MR1* locus
687 of GBM and high-grade glioma samples, GBM2w (IDHwt GBM, GSM1824806), AA15m
688 (IDHmut-R132H, Grade3 Astrocytoma, GSM1824808). (e) Single-cell RNA-seq data of 3589
689 cells from GBM tissues of four patients were analyzed with a tSNE plot. All colored dots represent
690 cells expressing *MR1*.

691

692 **Figure_2**

693 **Correlations of *MR1* expression and the activity of TANs/MDSCs**

694 (a) A schematic illustration of the extracted top 500 significantly co-expressing genes with *MR1*
695 and the prognosis related 158 genes among them. The horizontal axis is the Spearman's *r* values
696 for each gene's correlation level with *MR1*, and the vertical axis is the *q*-value (Benjamini-
697 Hochberg adjusted *p*-value) for each gene. (b) The enriched pathways of the 158 genes. The bar
698 chart shows the enriched *q*-values for each pathway. (c) Correlation scatter charts between *MR1*
699 gene expression, NDsig-index, and MDSCsig-index among the 168 TCGA-GBM samples.

700

701 **Figure_3**

702 **Multi-faceted evaluation of the MAIT infiltrated samples in TCGA-GBM**

703 (a) The levels of MAIT-cell infiltration in TCGA-GBM samples. The 8.3% (14/168) of samples
704 were detected as MAIT cell infiltration positive samples. The infiltration level was calculated with
705 the formula, [The detected read count of the MAIT-target read of the sample/ The total RNA read
706 count of the sample]. (b)(c) Violin plots showing the gene expression level of MAIT cell surface
707 receptors/secreting cytokines. (d) The information on MAIT cell infiltration was integrated with
708 other clinical/molecular indicators. Molecular indicators' information was obtained from a
709 previously reported database[27], and the neural samples were integrated into the proneural samples.
710 (e) The ratio-bar chart shows the distribution of GBM subtypes among MAIT-positive samples
711 and the total TCGA-GBM samples. (f) A violin plot showing the *MR1* gene expression level in
712 the MAIT positive/negative groups.

713

714 **Figure_4**

715 **Evaluations of the activity of TANs/MDSCs in MAIT-positive/negative samples**

716 (a) The enrichment plot of GSEA-GOBP's negative regulation of immune response in MAIT-
717 positive/negative samples. (b) The enrichment results of neutrophil-related pathways in GSEA-
718 GOBP in MAIT-positive samples. All pathways shown were significantly enriched ($q < 0.05$). (c)
719 Heatmap of the gene expression level of ND30 genes for each sample. The vertical column
720 represents one GBM sample. MAIT-positive samples were gathered on the right. (d) A Violin plot
721 showing the ND30-index level. (e) GSEA enrichment plots of neutrophil degranulation pathway
722 and MDSC signature. (f) Scatter chart showing the differential expression levels of the
723 immunosuppressive pathway genes related to TANs/MDSCs among MAIT-positive/negative

724 samples. The horizontal axis shows the fold change (log2 converted) as follows. [Mean FPKM of
725 MAIT-positive samples / Mean FPKM of MAIT-negative samples] The vertical axis shows the *p*-
726 value (-log2 converted) of the unpaired t-test that compares the expression levels of MAIT-
727 positive/negative samples for the gene. (g) Violin plots showing the *ASS1* or *ARG1* gene
728 expression level. (h) Violin plots showing the expression level of *FOXP3* and *CCR4*. (i) GSEA
729 enrichment plot, using our Treg-signature gene set. (j) The prognostic correlation of NDsig-index
730 and MDSCsig-index with TCGA-GBM clinical data. Cut off: NDsig-index = 41.89, MDSCsig-
731 index = 27.48, Log-rank test
732
733 **Figure_5**
734 **Correlations between *MR1*, prognosis, and TANs/MDSCs in the pan-cancer analysis**
735 (a) The prognostic correlation of *MR1* in multiple cancer types. All red lines represent the MR1-
736 high group, and blue lines represent the MR1-low group. (b) Enrichment plots of the GSEA using
737 neutrophil degranulation pathway and our MDSCsig gene set for multiple cancer types. MR1-
738 high/low groups were compared. (c) The enrichment results of neutrophil related pathways in
739 GSEA-GOBP in the MR1-high group. All pathways shown were significantly enriched ($q < 0.05$).
740
741 **Figure_6**
742 **The MAIT/MR1-TAN/MDSC pathway**
743 The activation of MAIT cell, along with the *MR1* up-regulation, activates and chemo-attracts
744 granulocytes, such as TANs/MDSCs, through IL-17 and TNF production. The activated
745 TANs/MDSCs induce Tregs via the production of TGF-β, CCL17, and CCL22, and Tregs suppress

746 the T cell-mediated immunity. Simultaneously, TANs/MDSCs suppress T cells via multiple
747 pathways. The suppression of T cell immunity provides a poor prognosis for GBM.

Supplementary figure

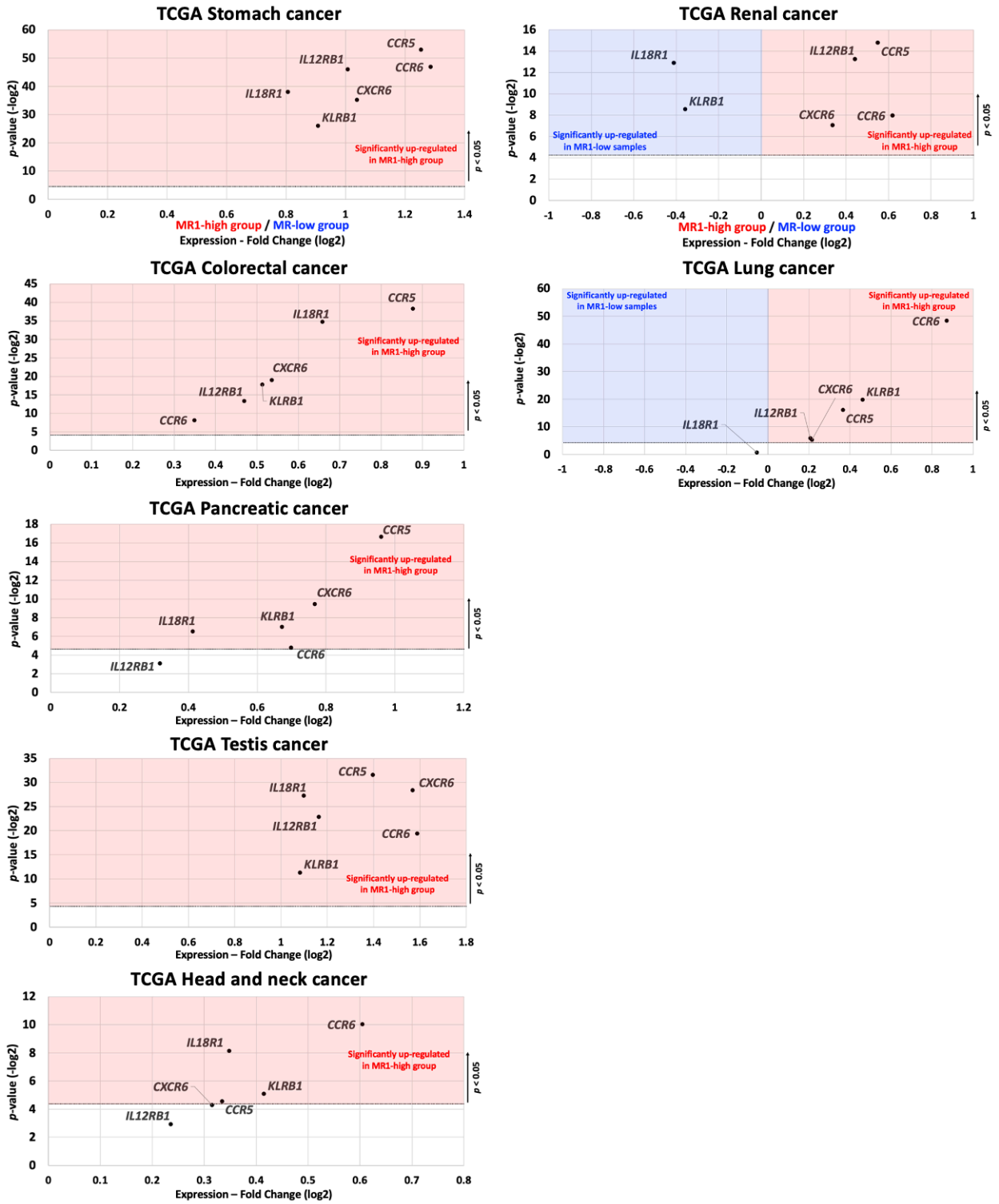

Figure_S1: The differential expressions of MAIT cell surface receptor genes in MR1-high/low group with pan-cancer analysis

Scatter charts show the differential expression levels of the MAIT cell surface receptor genes in the MR1-high/low group. The horizontal axis shows the fold change (log2 converted) as follows. [Mean FPKM of MR1-high group / Mean FPKM of MR1-low group] The vertical axis shows the significance (unpaired t-test).